An EPR Spin Label Study of the Quinol Oxidase, *E. coli* Cytochrome bo_3: A Search for Redox Induced Conformational Changes†

Gaye F. White,‡ Sarah Field,‡ Sophie Marritt,‡ Vasily S. Oganesyan,*,‡ Robert B. Gennis,§ Lai Lai Yap,§ Andromachi Katsonouri,§,|| and Andrew J. Thomson*,‡

School of Chemical Sciences and Pharmacy, University of East Anglia, Norwich NR47TJ, U.K., and Department of Biochemistry, University of Illinois, 600 South Mathews Street, Urbana, Illinois 61801

Received November 2, 2006; Revised Manuscript Received December 21, 2006

ABSTRACT: A search for conformational changes at the cytosolic entrance to the proton channels of the heme−copper quinol oxidase (QO), cytochrome bo_3, *E. coli*, has been carried out using site directed nitroxide spin labeling (SDSL) of cysteine residues. These were positioned at R134 and R309, on loops that link helices II and III and VI and VII at the entrances to the D and K proton channels, respectively. The motional characteristics of both labels have been determined using X- and W-band EPR spectroscopy at room temperature in selected redox levels in the reaction sequence of QO with oxygen, namely, the mixed valence carbon monoxide form (COMV), the oxidized (O) and super-oxidized (P_M) states. The O to P_M step is accompanied by the uptake of protons through the K pathway. We find no evidence for changes in the motional characteristics of either label that are expected to be associated with helical motions at the entrances to the channels. Because kinetic studies of mutants show that the redox gating of protons occurs deep within the D channel close to the heme−copper site, the present study implies that no motion is transmitted to the ends of the helices.

Heme−copper oxidases (HCOs[1]) are transmembrane proteins that catalyze the reduction of dioxygen to water in the aerobic respiratory chains of prokaryotes and in mitochondria (*1*). Most members of this family are redox driven proton pumps in which the free energy of oxygen reduction is coupled to the vectorial translocation of protons across the membrane (*2*). In the case of cytochrome *c* oxidase (CcO), electrons are supplied from cytochrome *c* via a copper center, Cu_A, whereas in quinol oxidase (QO), electrons come from quinone in the membrane, and consequently, the protein lacks a Cu_A center (*3*−*5*). All HCOs contain two heme groups: a *b*-type heme and a binuclear heme o_3−copper center, denoted heme-Cu_B, both located within the highly conserved subunit I, common to all HCOs, and formed by 12 trans-membrane helices. The reduction of di-oxygen takes place at the binuclear heme−copper center. On reaction with oxygen, the protein passes through a four electron oxidation−reduction cycle during which four protons are taken up from the electrically negative (N) side of the membrane into the oxygen binding site to generate water, and an additional four protons are transferred from the N to the positive (P) side. Two proton conducting channels, D and K, running from the N surface of the protein to the heme−copper binuclear site, have been identified by crystallography and from studies of mutant forms (*3*, *6*, *7*). The K channel is used for the uptake of one to two protons during the reduction of the binuclear site but not during the oxidation by O_2. The D pathway is used for the uptake of both the substrate and pumped protons. There is recent evidence of a branch point in the D channel from which protons are transferred either to the binuclear site, as substrate protons, or to a protonatable group in the output channel, as pump protons (*8*).

The reaction sequence of HCOs with O_2 has been well established (*1*). In the reduced, R, state the heme *b* is in the low spin ferrous form, Fe(II), and the binuclear, heme-Cu_B center contains high spin ferrous heme, Fe(II) and Cu_B(I). O_2 rapidly binds to the binuclear center to form the A state, which contains Fe(II)-(O_2)-Cu_B(I). This is followed by reduction and scission of the O−O bond, leading to the formation of a four electron oxidized state, denoted P_M. In this state, heme *b* is in the low spin ferrous form, and the binuclear site contains ferryl heme (Fe(IV)═O) and Cu_B(II) plus an organic radical, Y•O, possibly the tyrosine residue covalently linked to one of the histidine ligands of Cu_B. Consecutive electron transfer then takes place into the binuclear site to generate first the F and then the O forms,

† This work has been supported by the UK BBSRC grants B17596 and B03637. We also thank the Wellcome Trust for a Joint Infrastructure Fund Award for equipment and running costs. V.S.O. thanks the EPSRC for an Advanced Fellowship.

* To whom correspondence should be addressed. Tel: 44-(0)1603 593051. Fax: 44-(0)1603-593045. E-mail: a.thomson@uea.ac.uk (A.J.T.); v.oganesyan@uea.ac.uk (V.S.O.).

‡ University of East Anglia.

§ University of Illinois.

|| Current address: Environmental Chemistry and Control of Effluents Laboratory, State General Laboratory, 44 Kimonos Street, 1451 Nicosia, Cyprus.

[1] Abbreviations: bo_3, *E. coli* cytochrome bo_3; CcO, cytochrome *c* oxidase; HCO, heme−copper oxidase; QO, quinol oxidase; CF, cysteine-free; WT, wild type; R, reduced; MVCO, CO-bound mixed valence; O, oxidized; P_M, dinuclear site four electron oxidized above the reduced state; P_R, dinuclear site three electron oxidized above the reduced state; AEBSF, 4-(2-aminoethyl)benzenesulphonyl fluoride; EDTA, ethylenediamminetetra-acetate; IMAC, metal ion affinity chromatography; LB, Luria broth; MTSL, (1-oxy-2,2,5,5-tetramethyl pyrrolidin-3-yl) methyl methanethiosulphonate; OD, optical density.

10.1021/bi062265h CCC: $37.00
Published on Web 02/09/2007

ferryl heme (Fe(IV)═O)-Cu_B(II) and high spin ferric heme Fe(III)-Cu_B(II). These steps are accompanied by the uptake of protons through the D pathway. The reduction back to the R state requires the transfer of two more electrons and two protons, which takes place via the K channel.

During the process of O_2 reduction, high pK_a proton acceptors are created at the catalytic site. Initially, these proton acceptors are protonated as a result of intramolecular proton transfer from a residue located in the membrane-spanning part of the enzyme but removed from the catalytic site. This residue is then re-protonated from the bulk solution. If this residue has a kinetic preference to accept a proton from a donor on the N side of the membrane when its pK_a is raised and to donate a proton to an acceptor group on the P side of the membrane after its pK_a has been lowered, then a proton is pumped across the membrane. Evidence points to residue E286 as the internal proton donor group that undergoes the pK_a shift, suggesting that this is the branch point at which protons are switched (*7*). However, it is known that the proton pump can be disabled by mutations at the entrance to the D channel. For example, in CcO from *Rhodobacter sphaeroides* the mutation Asn139 to Asp uncouples the pump from catalytic turnover even though the perturbation is some 20 Å from E286 (*2*).

In this article, we describe experiments in which EPR nitroxide spin labels have been attached to cysteine residues at two different positions on the N side of the protein. The cysteine residues have been individually engineered in place of natural residues, in the vicinity of the entrances to the D and K channels, to serve as probes of conformational changes remote from the heme−copper site (*9*−*11*). A doubly labeled mutant was also prepared to investigate the detection of distance related dipolar interactions between spin labels (*12*, *13*). Spin labels can be covalently attached to the side chains of cysteine residues positioned by site directed mutagenesis (*14*). The nitroxide label introduces a relatively stable unpaired electron with slow electron spin relaxation compared to that of transition metal ions, thereby allowing the detection by EPR at room temperature. At X-band (9.5 GHz), the EPR of the NO• group shows a three-line spectrum, centered at $g = 2.0$, which arises from hyperfine coupling of the electron to the ^{14}N ($I_N = 1$) nucleus (*15*, *16*). Higher resolution is achieved at W-band (95 GHz), and at this frequency, both *g*-factor anisotropy and hyperfine coupling can be observed in the spectrum of the spin label. At room temperature, relative motions of the nitroxide label and the protein, such as overall tumbling and local backbone fluctuations, influence the dynamics of the spin label that affect the EPR spectral line shapes (*17*). When EPR spectra at two well separated frequencies, such as X- and W-bands, are available, the analysis of these motional effects can be clarified (*18*−*21*). We have sought changes to the motional freedom of spin labels on cycling the protein through the following states, namely, the reduced (R), the CO-bound mixed valence (COMV), the fully oxidized (O), and the four electron oxidized (P_M) states. In this study, we elected to study the quinol oxidase, cytochrome bo_3, found in the inner membrane of *Escherichia coli* because it lacks the center Cu_A, which has EPR signals in the $g = 2.0$ region in the oxidized state overlapping the spectral region where nitroxide spin label signals are observed. A crystal structure of *E.coli* cytochrome bo_3 is available (*3*). Figure 1 shows the structure of subunit I where the redox centers and proton pumping channels are located.

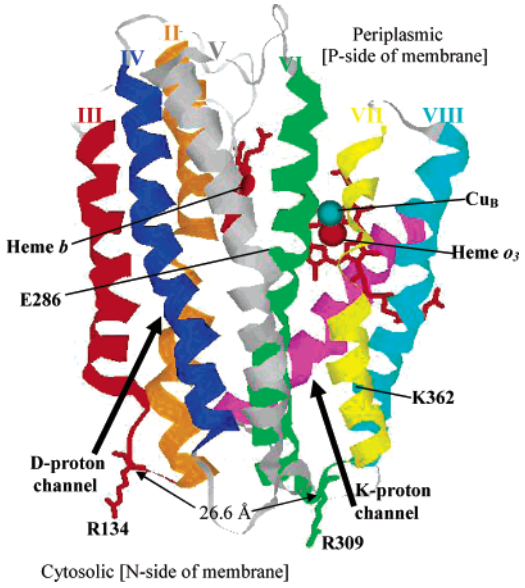

FIGURE 1: X-ray crystallography structure of subunit I of *E. coli* cytochrome bo_3. The distances between residues (between Cα's and from Cα to the metal ion center) have been estimated as R134−R309 = 26.6 Å, R134−heme *b* = 37.3 Å, R134−heme o_3 = 35.3 Å, R134−Cu_B = 36.2 Å, R309−heme *b* = 35.4 Å, R134−heme o_3 = 33.5 Å, and R134−Cu_B = 31.7 Å.

All nine cysteine residues in WT *E. coli* cytochrome bo_3 were removed genetically to create a cysteine free (CF) form. Cysteines were then engineered back into positions selected for spin labeling. The positions chosen were R134 and R309; see Figure 1. Helices II, III, and IV form the D channel. R134 lies at the center of a loop joining the ends of helices II and III, adjacent to the conserved aspartic acid residue D135 that is essential for proton transport into this channel. R309, however, is on a loop linking helices VI and VII close to the entrance to the K channel, which is formed by helices VI, VII, and VIII. The conserved residue K362, which gives its name to this channel, lies two helical turns into the channel. The double mutation R134C, R309C was also constructed. The distances of the Cα carbon atoms from the Fe atom in the centers of hemes *b* and o_3 and from Cu_B are given in the Figure as are the distances between the Cα atoms of residues 134 and 309.

EXPERIMENTAL PROCEDURES

Preparation of Cytochrome bo_3. Cytochrome bo_3 was expressed in *E. coli* BL21 strain Δcyo recA$^-$, which carries a deletion of the chromosomal bo_3 gene to prevent recombination and is kan^{50} tet^{15} resistant, according to the method of Rumbley et al. (*22*). The construction of the plasmid used to express his tagged cytochrome bo_3 is also described in this reference. Cells were prepared from fresh transformations using freshly made competent cells before each grow up. Expression was checked using Western blot of overnight culture from the transformation plate. Cells were grown in 2l $LB_{kan,tet,amp}$ baffled flasks supplemented with 0.3% sodium lactate (60% w/v syrup) and 0.5 mM $CuSO_4$. The medium was innoculated with 10 mL of healthy overnight culture followed by growth to 0.8−1.1 OD_{600} at 37 °C. Cells were harvested by centrifugation at 6000 rpm for 15 min at

4 °C, resuspended in resuspension buffer 1 (see buffers listed below) then broken by French pressing. Unbroken cells were removed after spinning at 13000 rpm for 20 min at 4 °C, and then the membrane portion was spun down by centrifugation at 45000 rpm for 60 min at 4 °C. The membranes were resuspended in resuspension buffer 2. 1% dodecyl maltoside was added and the mixture stirred for 60 min at 4 °C. Unsolubilized material was removed by centrifugation at 45000 rpm for 60 min at 4 °C. The solubilized material was loaded onto a Ni^{2+} charged IMAC column. The column was washed with 6 column volumes of column buffer A followed by 40 column volumes of a high salt buffer. The protein was eluted with an A−B buffer gradient over 15 column volumes. Purity was assessed by SDS−PAGE, using silver and Coomassie staining. The product, oxidized cytochrome bo_3, was concentrated by Amicon ultra-filtration and the protein concentration determined from the absorbance of the Soret band, $\epsilon^{406} = 182$ mM^{-1} cm^{-1} for oxidized cytochrome bo_3 (*23*).

Resuspension buffer 1 consisted of 50 mM K_2HPO_4 at pH 8.3 + 5 mM $MgSO_4$, 1 mM AEBSF protease inhibitor (4-(2-aminoethyl)benzenesulphonyl fluorine HCl), 2 mM benzamide, and 4 mg L^{-1} DNase. The buffer was made using K_2HPO_4 and was pH adjusted with 50 mM KH_2PO_4. Resuspension buffer 2 consisted of 50 mM K_2HPO_4 at pH 8.3 and column buffer A of 50 mM K_2HPO_4 at pH 8.3, 25 mM imidazole, and 0.1% dodecyl maltoside. High salt buffer was made up of 250 mM K_2HPO_4 at pH 8.3, 25 mM imidazole, and 0.1% dodecyl maltoside. Column buffer B consisted of 50 mM K_2HPO_4 at pH 8.3, 300 mM imidazole, and 0.1% dodecyl maltoside and column strip buffer of 50 mM K_2HPO_4 at pH8.3, 25 mM imidazole, and 50 mM EDTA.

Preparation of Single and Double Mutants R134C, R309C, and R134C/R309C. Site directed mutagenesis was used to modify the amino acid sequence encoded by the cytochrome bo_3 plasmid so that the nine naturally occurring cysteine residues in *E. coli* cytochrome bo_3 were removed to create a cysteine free (CF) form. The single point mutations R134C and R309C and the double mutations R134C, R309C were then introduced into the CF form. Each cytochrome bo_3 variant was prepared as described above and analyzed for reactive thiol content using a Molecular Probes thiol and sulfide quantification kit. The activity of the mutant proteins was verified by monitoring the oxidation of decyl-ubiquinol following the method described by Rumbley et al. (*22*).

Preparation of Spin Labeled Cytochrome bo_3 in Various Oxidations States . Concentrated samples of purified enzyme were incubated with the sulfydryl-specific nitroxide spin label MTSL, (1-oxy-2,2,5,5-tetramethyl pyrrolidin-3-yl) methyl methanethiosulphonate, at a 2-fold concentration over the labeling site. Incubation was performed at either room temperature for 4 h or overnight at 4 °C. Initially, excess spin label was removed by passage through 2 Sephadex G-25, PD10 columns (obtained from Amersham Biosciences, U.K.). Using this procedure, there was evidence from the EPR spectra for a background of nonspecifically bound label in the cysteine free variant. This background may have some contribution from the label trapped within the dodecyl maltoside detergent vesicles or from impurities not removed by the protein purification method. The following method was used to exchange the protein into fresh detergent buffer following spin labeling. Excess label was removed by washing on a small metal ion affinity chromatography (IMAC) column prepared from nickel ion loaded Chelating Sepharose Fast Flow material, equilibrated with 50 mM potassium phosphate, 25 mM imidazole at pH 8.3, and buffer containing 0.1% (w/v) dodecyl maltoside. The spin labeled sample was diluted with the equilibration buffer, loaded onto the column and washed with 6 column bed volumes of equilibration buffer followed by 20 bed volumes of 250 mM potassium phosphate, 25 mM imidazole at pH 8.3, and 0.1% dodecyl maltoside buffer. Clean spin labeled enzyme was eluted with 50 mM potassium phosphate, 300 mM imidazole, pH8.3, 0.1% dodecyl maltoside buffer, followed with buffer exchange by ultrafiltration to remove the imidazole. Fractions containing pure cytochrome bo_3 were pooled, concentrated and excess imidazole removed by further ultrafiltration washes.

Preparation of the COMV and P_M Forms. The mixed valence CO-bound form of cytochrome bo_3 provides convenient access to the P_M state. When an oxidized sample of cytochrome bo_3 is held under an atmosphere of CO, the binuclear heme−copper center is reduced to heme o_3-CO plus Cu_B(I), leaving heme *b* in the low-spin Fe(III) state. The CO ligand is removed by photolysis in the presence of O_2, causing the heme−copper site to undergo a four electron oxidation to the P_M state. A freshly labeled sample of cytochrome bo_3 exchanged into 25 mM bis-tris propane at pH8, 0.1%w/v dodecyl maltoside, and buffer was transferred to a suba-sealed bijou bottle, with a needle outlet, and stirred under a flow of nitrogen for 30 min. The bijou bottle was covered with foil to exclude light prior to exchanging the gas flow with carbon monoxide. The sample was stirred under CO gas flow for 10 min and then for 45 min under the CO atmosphere in the sealed bottle. The sample was transferred to a sealed cuvette containing CO, excluding all light during sample manipulation. CO binding was monitored by a shift in the Soret band to 414 nm, increased intensity of bands at 533 and 564 nm, and quenching of the charge transfer band at 630 nm. The difference spectrum with respect to the oxidized form shows peaks at 535 and 565 nm and a trough at 630 nm, giving a spectrum characteristic of the MV-CO form. The P_M form was generated from the MV-CO enzyme by exposure to air followed by irradiation from a slide projector lamp. The optical absorption difference spectrum with respect to the oxidized spectrum shows a shift back of the Soret to 410 nm, peaks at 530 and 560 nm, and some recovered intensity at 630 nm. The sealed cuvette was transferred to an anaerobic glove box operating at typically less than 3 ppm oxygen level. Five microliters of the MV-CO sample was transferred, in the dark, via a syringe into a capillary EPR tube for X-band EPR measurement at room temperature. Samples for low-temperature X-band EPR experiments were transferred directly from the sealed vial to the EPR tube and frozen in liquid nitrogen.

Preparation of Reduced Samples of Spin Labeled Cytochrome bo_3. The reduction of spin labeled cytochrome bo_3 needs care to avoid reduction of the nitroxide NO bond of the spin label itself, which has a potential of ~10 mV. Thus, reduction was effected with previously electrochemically reduced duroquinol. Freshly prepared aliquots of duroquinol were added to anaerobic samples of cytochrome bo_3 labeled with MTSL. Reduction was monitored by absorption spec-

troscopy. Between 2 to 3 mol equiv of duroquinol were titrated until the reduction of heme o_3 was complete, as judged by the disappearance of the 630 nm charge transfer band.

EPR Spectroscopy. Room-temperature X-band EPR spectra were acquired using a Bruker EleXsys 500 spectrometer fitted with an ER4123D resonator with samples contained in 0.6 mm id × 0.84 mm od quartz tubes. Room-temperature W-band, EPR spectra were acquired using a Bruker EleXsys 680 spectrometer with samples contained in 0.1 mm id × 0.5 mm od quartz tubes. A Bruker EleXsys 580 system with an ER4118X-MD resonator was used in the continuous-wave mode to record X-band EPR at 170 K.

Simulation of Room-Temperature EPR Spectra. Simulations of EPR spectra were performed using the module EPRSSP_DYN of an EPR computer simulation program developed by VSO. The method, which has been described elsewhere (*24*), is based on the direct numerical simulation of CW EPR spectra of nitroxide spin labels from Brownian rotational dynamics trajectories of protein and spin label orientations, first described by Robinson et al. (*25*). In brief, the contributions to the EPR absorption spectra are given by the Fourier transform of the transverse magnetization trajectory of the spin label generated at each initial position in space. The transverse magnetization curve for each of the three hyperfine lines of a nitroxide spin label is calculated using the following integral form:

$$\langle M_+^m(t)\rangle = \langle M_+^m(0)\rangle \exp\left(-\left[i\int_0^t \hbar\omega^m(\tau)d\tau + \frac{t}{T_2^m}\right]\right) \quad (1)$$

where the Larmor frequencies for the three hyperfine lines and $\omega^m(t)$ are functions of the orientation trajectory $\Omega(t)$ according to eq 2.

$$\hbar\omega^m(t) = g_{ZZ}(\Omega(t))\,\beta B + A_{ZZ}(\Omega(t))m \quad (2)$$

Here, B is the value of magnetic field, and m is the projection of the nitrogen nuclear spin on its quantisation axis, which is equal to ±1.0 for ^{14}N. g_{ZZ} and A_{ZZ} are effective g- and A-values of nitroxide spin label at time t. The time dependent fluctuation of $\omega^m(t)$ is caused by Brownian motion. This fluctuation is associated with the correlation time, τ, of the Brownian dynamics of the spin label. A special normalized correlation function is used in the equation for A_{ZZ} to account for the time averaging of the pseudosecular terms in the spin-Hamiltonian because of reorientational motion, as described previously (*26*). Completely motionally averaged spectra are obtained when the correlation time is short, compared to the inverse microwave frequency used in the EPR measurements $\tau \ll 1/\nu_0$, and the rigid limit spectrum is achieved in the opposite case $\tau \gg 1/\nu_0$. In the simple case of the single isotropic rotational diffusion of a label, the correlation function will decay exponentially, but when other types of motions, such as protein rotational diffusion, are included, a multimodal dependence is found. In general, correlation times provide a measure of spin correlation decay. In order to account for homogeneous line broadening of the EPR spectrum, the transverse relaxation time T_2^m is introduced.

Our program considers the most general case in which the overall spin label motion is the superposition of Brownian rotational diffusion of the protein and the independent motion of the spin label. These are described by two rotational diffusion tensors characterized by principle values and orientations. The restricted motion of a label is modeled by a numerical solution of the Langevin equation for stochastic rotational dynamics of a single particle in the presence of an ordering potential (*27*). The dynamics are approximated by a particle undergoing a Brownian rotational motion exposed to the mean force of a restricted potential imposed by the protein. For an axially symmetric restoring potential along a direction relative to the protein domain, the type of label motion is associated with an order parameter S (*17*), calculated from the dynamical trajectories generated according to the following equation

$$S = 1/2(3\langle\cos\beta^2\rangle - 1) \quad (3)$$

where β is the angle between the z-axis of the spin label and the vector of the mode of the motion directed along the minima of a restricted potential in the protein domain. The average is taken over all dynamical trajectories and all points of time along the trajectory until the rotational correlation function relaxes. When $S = 1$, the label is rigid, and when $S = 0$, the labels are rotating isotropically (*17*).

Numerical solutions of the Langevin equation provide the orientation trajectory for the nitroxide label, which should be long enough (usually microseconds) to ensure sufficient resolution for the Fourier transformation. Finally, the total line shape intensity is averaged over all possible initial orientations with the proper equilibrium distribution. For the range of correlation times used in this article, 400 Brownian trajectories and 900 initial points within the octant of a unit sphere were sufficient to simulate a spectrum with acceptable signal-to-noise level.

RESULTS

Room-Temperature EPR of Cytochrome bo_3 Spin Labeled at Entrances to D and K Proton Channels. Spin labels were attached to each of the single mutants, R134C and R309C, and the double mutant C134/C309 by reaction with MTSL followed by one of the two column chromatography procedures described in Experimental Procedures. The same experiments were performed on the CF variant to assess the degree of background labeling. Each eluant was concentrated prior to recording the room-temperature X-band EPR spectra. The protein concentrations were determined spectrophotometrically at the Soret band wavelength of 406 nm using $\epsilon^{406} = 182\ \mathrm{mM}^{-1}\ \mathrm{cm}^{-1}$. The extent of spin label attachment was determined by comparing the double integration of the room-temperature CW EPR spectrum to that obtained for an MTSL solution of known concentration. Ninety to 100% labeling efficiency was determined in every case. However, after 1−2 h of storage at 4 °C, a proportion of spin label became detached from the protein. This was detected as a sharp EPR spectrum characteristic of free MTSL superimposed on the broader EPR signal. Therefore, only the freshly spin labeled protein was used for the EPR experiments. After treatment with MTSL, the CF variant gave an EPR spectrum apparently arising from nonspecific binding to the protein or to an impurity. The intensity of this background varied

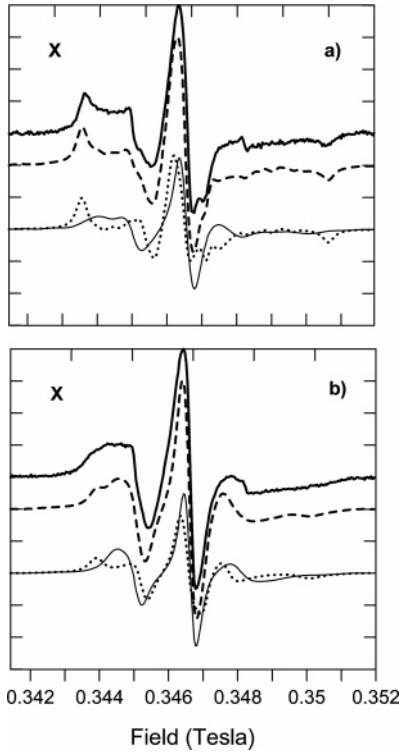

FIGURE 2: Room-temperature X-band EPR spectra of spin labeled bo_3 mutants (a) R134C and (b) R309C. Spectra were recorded at 295 K, 9.72 GHz, and 2 mW microwave power with 1 G modulation amplitude. In each case, the solid bold line is the experimental spectrum with the dashed line below showing the simulated spectrum, which is made up of two components represented by the lower fine solid and dotted lines.

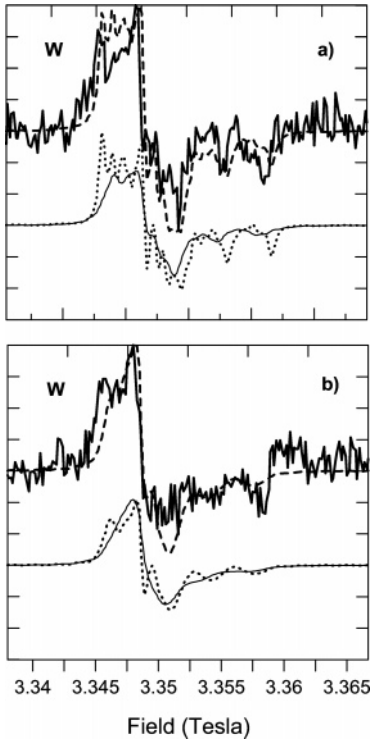

FIGURE 3: Comparison of room-temperature W-band EPR spectra of spin labeled bo_3 mutants (a) R134C and (b) R309C with line shapes predicted by using parameters obtained from simulations of the X-band spectra. Spectra were recorded at 295 K, 94.18 GHz, and 0.1 mW microwave power with 1 G modulation amplitude. In each case, the solid bold line is the experimental spectrum with the dashed bold line showing the simulated spectrum, which is made up of two components represented by the lower fine solid and dotted lines.

between batches of purified protein but was significantly reduced when a metal ion affinity column was used to exchange the protein into fresh detergent buffer after treatment with MTSL. Integrations of the EPR spectra recorded for the MTSL treated CF showed that the extra cleanup step reduced the background contribution due to nonspecific labeling from 25% to <10%. Therefore, this cleanup technique was routinely used for all the spin labeled protein preparations reported in this work.

The room-temperature CW X-band EPR spectra of cytochrome bo_3, singly labeled at C134 and C309, are shown in Figure 2. The spectral lineshapes are distinctive for each spin label site. In order to broaden the dynamic range and aid the deconvolution of motional effects influencing the nitroxide EPR, room-temperature W-band spectra were also obtained (Figure 3). The S/N ratio is less than optimal because the protein concentration of cytochrome bo_3 in detergent is difficult to increase above 150 μM without precipitation. Nevertheless, the spectra give useful information that augments that obtained at X-band.

Analysis of Spin Label Motion. In order to determine the motional parameters for spin labels at positions C134 and C309, the line shapes of the room-temperature X-band spectra were simulated using the method described in Experimental Procedures. Room-temperature W-band spectra were then simulated using the motional parameters determined at X-band. The experimental spectra and the simulations are shown in Figures 2 and 3. Using the Brownian dynamics model in the simulation, we have been able to reproduce all the essential features of the EPR spectra, which are characteristic of a particular type of motion, using a minimal set of adjustable parameters. For the sake of simplicity, the bandwidth, defined by the transverse relaxation time T_2, is assumed to be isotropic and independent of hyperfine coupling. This assumption reduces the number of adjustable parameters required to achieve satisfactory fits of the experimental spectra. Although improved fits could be achieved by variation of bandwidth parameters, this would not add extra information.

A comparison of the simulated spectrum with the experimental spectrum observed for the spin label on C134 at X-band is given in Figure 2a. The protein rotational diffusion is too slow to be detectable in the spectra on the time scales of X- and W-band frequencies and has not, therefore, been included in the simulations. The motional parameters obtained show that the spin label on C134 has two modes of motion with almost equal contributions. The first, accounting for 60% of the total spin, is associated with a highly restricted label motion with parameters $\tau_c(x) = \tau_c(y) = \tau_c(z) = 1$ns and $S = 0.90$ for the axially symmetric potential along the z-axis of the nitroxide spin label. This corresponds to an almost completely frozen label. The second mode, about 40% of the label, is less strongly immobilized and is described by the parameters $\tau_c(x) = \tau_c(y) = \tau_c(z) = 4$ ns and $S = 0.55$. The presence of the second mode is responsible for the intensity observed in the EPR X-band spectrum between 3435 and 3450 G as can be seen from the de-convolution of the spectrum. In addition, a plateau observed in the spectrum between 3475 and 3480 G is due to a cancellation effect

between positive and negative features of the second and first motional modes, respectively. The experimental spectrum at X-band also shows the presence of a small contribution from free spin label giving rise to the high field sharp derivative feature at approximately 3483 G. This arises from the unbound label and has not been taken into account in the simulation. Apart from this, the X-band simulation fits all of the features observed in the experimental spectrum. The validity of the motional parameters is corroborated by the room-temperature W-band spectrum (Figure 3a). This Figure shows the W-band line shapes predicted using parameters obtained from simulations of the X-band spectrum.

Simulation of the X-band EPR spectrum observed for the spin label on C309 (Figure 2b) also reveals two modes of motion contributing equally to spectra at both X-band and W-band (Figure 3b). As in the case of SLC134, both modes are associated with the Brownian diffusion of a label in an axially symmetric ordering potential with the symmetry axis along the *z*-axis of the hyperfine coupling tensor. Parameters for one contribution at 50% of a spin are $\tau_c(x) = \tau_c(y) = \tau_c(z) = 2$ ns and order parameter $S = 0.45$. For the other contribution, also at 50%, the parameters were $\tau_c(x) = \tau_c(y) = \tau_c(z) = 2$ ns and order parameter $S = 0.63$. Once again, there is a very small amount of free spin label detected at 3483 G that has not been taken into account in the simulation.

In both cases, protein motion, including tumbling, is slow compared to the time scale of the microwave frequencies used in EPR experiments and, therefore, does not affect the shapes of either X- or W-band EPR spectra. The simulations showed that both X- and W-band spectra can be fitted equally well with and without the inclusion of overall protein rotational diffusion with correlation times >80 ns, the overall motion expected for a large protein in a detergent micelle. Indeed, the M_r of cytochrome bo_3 is about 160 KDa, which according to the simple relationship, τ_c in $ps \approx M_r$, provides an approximate value for the rotational diffusion correlation time of the protein of ~160 ns. For both spin label sites, the analysis of the spin label EPR spectra indicates two conformers that have different axially symmetric ordering potentials measured by the parameter, *S*. In the case of the spin label on C309, each conformer has a rather similar *S* value of 0.45 and 0.63. However, in the case of the spin label on C134, the order parameters are 0.55 and 0.90, indicating one conformer with mobility similar to that of the C309 conformers and one of very restricted mobility. In both simulations, the rotational diffusion correlation times, τ, of the spin label vary between 1 and 4 ns. Although both sites C134 and C309 are on loops on the N side of the protein linking two helices close to the mouth of a proton conducting channel, the surface motions of the spin labels are restricted in different ways. This must reflect the fact that the spin label motions are hindered in subtly different ways by the protein side chains that surround them, making them sensitive reporters of local changes in protein structure.

Room-Temperature EPR of Spin Labeled Cytochrome bo_3 as a Function of Oxidation State. The room-temperature X-band EPR spectra have been measured for spin labeled cytochrome bo_3 in four different oxidation states, namely, the reduced (R), CO-bound mixed valence (COMV), and P_M and oxidized (O) states. These redox states pass the protein through part of the cycle in which protons are taken up and pumped. The EPR spectra have been measured at low temperatures between 5 and 20 K and a variety of powers in order to ascertain that the heme and heme−copper oxidation states are correct and to quantify them. Heme b is detectable at $g = 2.98$, 2.24, and 1.50, and the coupled HS heme Fe(III) o_3-Cu_B(II) shows a broad signal between g ~3 and 4. The metal centered spins have also been quantified in this way (*23*).

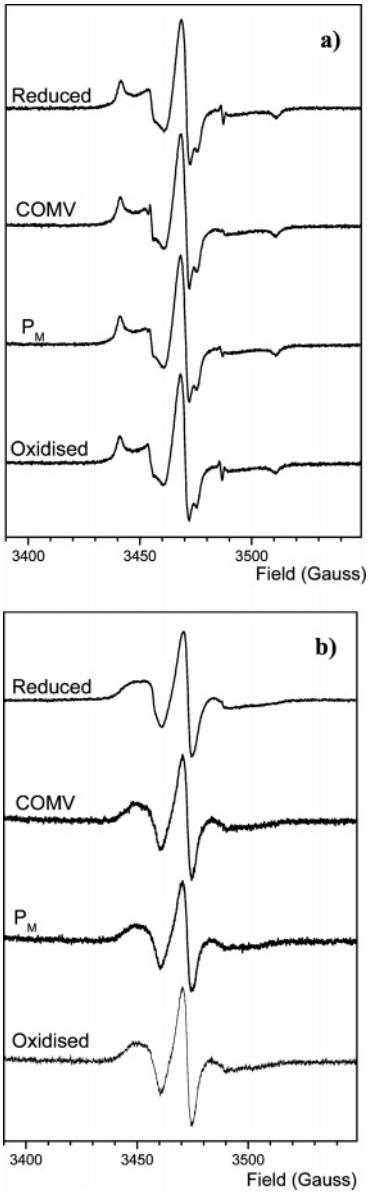

FIGURE 4: Room-temperature X-band EPR spectra of spin labeled bo_3 mutants (a) R134C and (b) R309C prepared in different oxidation states: R, COMV, P_M, and O. Spectra were recorded at 295 K, 2 mW microwave power with 1 G modulation amplitude, and frequency = 9.72 GHz.

The RT EPR spectra recorded for spin labeled cytochrome bo_3 R134C are shown in Figure 4a, and those of spin labeled cytochrome bo_3 R309C are given in Figure 4b. The spectra have been normalized in intensity at the major peak to allow line shape comparisons. Apart from slight changes in the narrower hyperfine regions, attributed to chemical release of the spin label from the protein, the spectra are identical in all four oxidation levels. Hence, no change in spin label motional characteristics were detected at either residue 134 or 309 on oxidizing from the MV-CO state to the P_M and O

forms. Therefore, using the spin labels as motional probes, no conformational changes associated with these redox changes can be detected in the loop regions near the entrances to either the D or the K channel.

Low-Temperature EPR of Singly and Doubly Labeled Cytochrome bo_3. If two spin labels are in close proximity, then dipolar exchange interactions between them can result in spectral broadening. Such effects are strongly distance dependent as the magnitude of the coupling depends upon $((1-\cos^2\theta)/R^3)$, where R is the distance between the magnetic electrons. Direct relationships between R and spectral broadening have been determined for two spin labels separated by distances in the range 10 to 25 Å (*12*, *27*). In order to discount motional effects, dipolar broadening is determined from frozen state EPR spectra. To investigate the possibility of observing dipolar coupling between spin labels attached at positions 134 and 309 on cytochrome bo_3, comparisons were made between low-temperature X-band EPR spectra of the singly and doubly labeled mutants, R134C, R309C, and R134C/R309C (Figure 5). As before, the experiment was carried out for the spin labeled cytochrome bo_3 mutants prepared in four different oxidation states: R, COMV, P_M, and O. The EPR line shapes did not vary between mutants and did not change when different oxidation states were prepared. In order to demonstrate this, Figure 5 shows the results obtained only for the P_M and O states. Room-temperature EPR spectra of the singly and doubly labeled mutants were also compared (results not shown). In this case, the summed spectra of the singly labeled mutants gave a line shape identical to that of the doubly labeled mutant.

Because molecular rotational motions are frozen at 170 K, it is not surprising that spin labels attached at 134 and 309 have identical low-temperature EPR spectra. It has been reported that differences in hyperfine splitting features may be observed if spin label environments differ in polarity (*19*). This does not appear to be the case for these labels. This is a reasonable result because as both are attached to loops at the N side of the protein, they are likely to be in similar environments. Because the EPR line shapes observed for the doubly labeled mutant match the sums of the EPR line shapes given by the singly labeled mutants, there is no evidence for dipolar coupling between labels on positions 134 and 309 in any of the oxidation states examined. This suggests that the distance between the nitroxide radicals is always greater than ~25 Å.

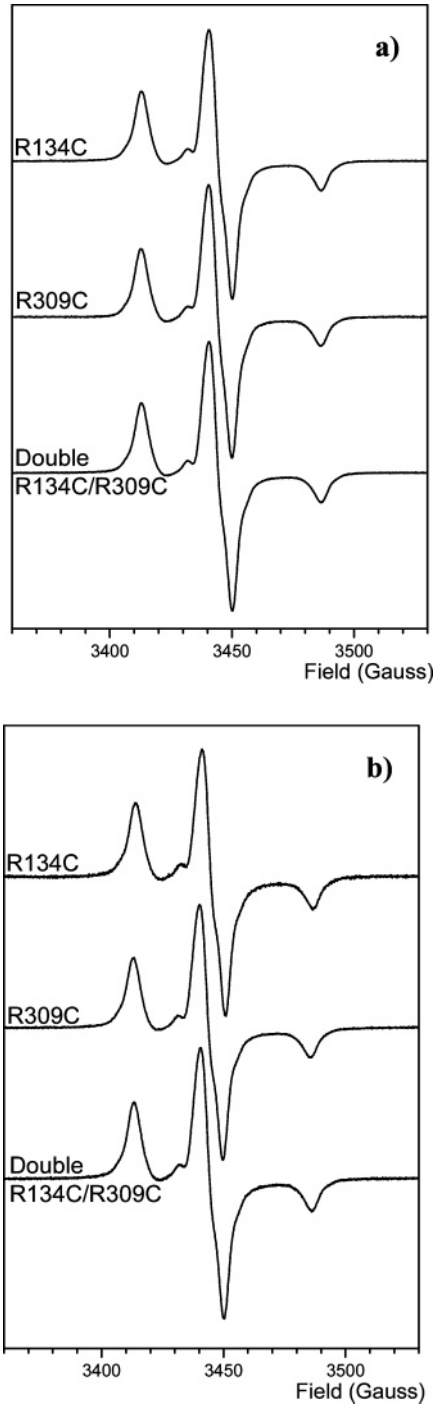

FIGURE 5: Low-temperature X-band EPR spectra of singly and doubly labeled bo_3 mutants, R134C, R309C, and R134C, R309C, prepared in different oxidation states. (a) Four electron oxidized (P_M); (b) fully oxidized (O). Spectra were recorded at 170 K, 0.006 mW microwave power with 1G modulation amplitude, and frequency = 9.65 GHz.

CONCLUSIONS

Pumping mechanisms in proteins should be accompanied by mechanical movement of the protein. So far, crystallographic evidence for redox dependent protein conformational changes in heme−copper oxidases has been lacking. X-ray crystallographic studies of the structures of bovine CcO in the O and R forms (at 2.30 and 2.35 Å, respectively) (*32*) and of the bacterial *P. denitrificans* CcO at 3.0 and 3.3 Å (*33*) found no significant differences in protein structure around the redox metal centers in subunit I. However, unstable intermediate states such as the P states, P_M or P_R, have not been studied by X-ray crystallography. These highly oxidized forms represent one of the extremes of the pump cycle and might be expected to show structural differences from, for example, the R form, the other cycle extreme. Alternatively, changes may be too small to be detectable at current levels of crystallographic resolution. Hence, the need for spectroscopic methods to probe structural changes over a pump cycle. The motion of secondary structure elements such as helices can be envisaged. For example, helices may rotate, one relative to another, causing the diameter of a channel to open and close like an iris, or they may undergo a piston-like motion directed along the axis of the helix. Motions of both types might be expected to lead to changes

at the loops linking the ends of the helices affected and, hence, should be reflected in the motions of the spin labels attached to them. Dynamic and conformational changes of this sort have been detected in several membrane proteins by spin label EPR (*27*−*29*). In the redox-active subunit I of cytochrome bo_3, the proton pumping channels lie within helical bundles. No changes in room-temperature EPR could be detected of spin labels attached at either position 134 or 309 that are situated on loops linking two helices that line the D and K channels as cytochrome bo_3 was passed through key states, O, R, and P_M, in its redox cycle. Thus, there is no evidence for changes in helical positions that might be associated with mechanical opening and closing of these channels as protons are pumped. A recent report using amide hydrogen/deuterium exchange in *Rhodobacter sphaeroides* (*RS*) CcO demonstrates that transitions between catalytic intermediates take place with the opening and closing of the D and K proton pathways, providing alternating access for protons to the two sides of the membrane (*31*). Interestingly, the peptide region between residues 123−135 in RS CcO (corresponding to cytochrome bo_3 residues 126−138) show no changes in D/H exchange kinetics as the enzyme cycles redox levels. This is consistent with the absence of any EPR line shape changes of SLC134 in cytochrome bo_3 as a function of the redox state. This work (*31*) does not report H/D exchange in the region of SLC309. Having established a protocol both for the spin labeling of cytochrome bo_3 and for the control of redox levels of spin labeled protein, it will be interesting to use SLs to probe the dynamics and polarity of the regions of CcO that have been shown to undergo alterations in deuterium exchange and, hence, water access during the operation of the proton pump.

REFERENCES

1. Brzezinski, P., and Larsson, G. (2003) Redox-driven proton pumping by heme-copper oxidases, *Biochim. Biophys. Acta 1605*, 1−13.
2. Namslauer, A., Pawate, A. S., Gennis, R. B., and Brzezinski, P. (2003) Redox-coupled proton translocation in biological systems: proton shuttling in cytochrome c oxidase, *Proc. Natl. Acad. Sci. U.S.A. 100*, 15543−15547.
3. Abramson, J., Riistama, S., Larsson, G., Jasaitis, A., Svensson-Ek, M., Laakkonen, L., Puustinen, A., Iwata, S., and Wikstrom, M. (2000) The structure of the ubiquinol oxidase from Escherichia coli and its ubiquinone binding site, *Nat. Struct. Biol. 7*, 910−917.
4. Hellwig, P., Barquera, B., and Gennis, R. B. (2001) Direct evidence for protonation of aspartate-75, proposed to be a quinol binding site, upon reduction of cytochrome bo_3 from Escherichia coli, *Biochemistry 40*, 1077−1082.
5. Grimaldi, S., MacMillan, F., Ostermann, T., Ludwig, B, Michel, H., and Prisner, T. (2001) Ubisemiquinone radical in the bo3-type ubiquinol oxidase studied by pulsed electron paramagnetic resonance and hyperfine sublevel correlation spectroscopy, *Biochemistry 40*, 1037−1043.
6. Verkhovskaya, M. L., Garcia-Horsman, A., Puustinen, A., Rigaud, J.-L., Morgan, J. E., Verkhovsky, M. I., and Wikstrom, M. (1997) Glutamic acid 286 in subunit I of cytochrome bo_3 is involved in proton translocation, *Proc. Natl. Acad. Sci. U.S.A. 94*, 10128−10131.
7. Lubben, M., Prutsch, A., Mamat, B., and Gerwert, K. (1999) Electron transfer induces side-chain conformational changes of glutamate-286 from cytochrome bo_3, *Biochemistry 38*, 2048−2056.
8. Branden, G., Gennis, R. B., and Brzezinski, P. (2006) Transmembrane proton translocation by cytochrome c oxidase, *Biochim. Biophys. Acta*, in press.
9. Hubbell, W. L., Machaourab, H. S., Altenbach, C., and Lietzow, M. A. (1996) Watching proteins move using site-directed spin labelling, *Structure 4*, 779−793.
10. Hubbell, W. L., Gross, A., Langen, R., and Lietzow, M. A. (1998) Recent advances in site-directed spin labelling of proteins, *Curr. Opin. Struct. Biol. 8*, 649−656.
11. Hubbell, W. L., Cafiso, D. S., and Altenbach, C. (2000) Identifying conformational changes with site-directed spin labelling, *Nat. Struct. Biol. 7*, 735−739.
12. Steinhoff, H.-J., Radzwill, N., Thevis, W., Lenz, V., Brandenburg, D., Anston, A., Dodson, G., and Wollmer, A. (1997) Determination of interspin distances between spin labels attached to insulin: comparison of electron paramagnetic resonance data with the x-ray structure, *Biophys. J. 73*, 3287−3298.
13. Persson, M., Harbridge, J. R., Hammarstrom, P., Mitri, R., Martensson, L.-G., Carlsson, U., Eaton, G. R., and Eaton, S. S. (2001) Comparison of electon paramagnetic resonance methods to determine distances between spin labels on human carbonic anhydrase II, *Biophys. J. 80*, 2886−2897.
14. Berliner, L. J. (1983) The spin label approach to labelling membrane protein sulfhydryl groups, *Ann. N.Y. Acad. Sci. 414*, 153−161.
15. Campbell, I. D., and Dwek, R. A. (1984) Electron Paramagnetic Spectroscopy, in *Biological Spectroscopy*, pp 179−215, Benjamin-Cummings, Menlo Park, CA.
16. Berliner, L. J. (1998) *Spin Labeling: The Next Millennium*, *Biological Magnetic Resonance*, Vol. 14, Plenum Press, New York.
17. Columbus, L., and Hubbell, W. L. (2002) A new spin on protein dynamics, *Trends Biochem. Sci. 27*, 288−295.
18. Barnes, J. P., Liang, Z., Machaourab, H. S., Freed, J. H., and Hubbell, W. L. (1999) A multifrequency electron spin resonance study of T4 Lysozyme dynamics, *Biophys. J. 76*, 3298−3306.
19. Steinhoff, H.-J., Savitsky, A., Wegener, C., Pfeiffer, M., Plato, M., and Mobius, K. (2000) High-field EPR studies of the structure and conformational changes of site-directed spin labelled bacteriorhodopsin, *Biochim. Biophys. Acta 1457*, 253−262.
20. Finiguerra, M. G., Van Amsterdam, I. M. C., Alagaratnam, S., Ubbink, M., and Huber, M. (2003) Anisotropic spin label mobilities in azurin from 95 GHz electron paramagnetic resonance spectroscopy, *Chem. Phys. Lett. 382*, 528−533.
21. Bennati, M., Gerfen, G. J., Martinez, G. V., Griffiths, R. G., Singel, D. J. and Millhauser, G. L. (1999) Nitroxide side chain dynamics in a spin labelled helix forming peptide revealed by high frequency (139.5 GHz) EPR spectroscopy, *J. Magn. Reson. 139*, 281−286.
22. Rumbley, J. N., Furlong-Nickels, E., and Gennis, R. B. (1997) One-step purification of histidine-tagged cytochrome bo_3 from *Escherichia coli* and demonstration that associated quinone is not required for structural integrity of the oxidase, *Biochim. Biophys. Acta 1340*, 131−142.
23. Cheesman, M. R., Oganesyan, V. S., Watmough, N. J., Butler, C. S., and Thomson, A. J. (2004) The nature of the exchange coupling between high-spin Fe(III) heme o_3 and CuB(II) in *Escherichia coli* quinol oxidase, cytochrome bo_3: MCD and EPR studies, *J. Am. Chem. Soc. 126*, 4157−4166.
24. White, G. F., Ottignon, L., Georgiou, T., Kleanthous, C., Moore, G. R., Thomson, A. J., and Oganesyan, V. S. (2007) Analysis of nitroxide spin label motion in a protein-protein complex using multiple frequency EPR spectroscopy, *J. Magn. Reson. 185*, 191−203.
25. Robinson, B. H., Slutsky, L. J., and Auteri, F. P. (1992) Direct simulation of continuous wave electron paramagnetic resonance spectra from Brownian dynamics trajectories, *J. Chem. Phys. 96*, 2609−2616.
26. Steinhoff, H.-J., and Hubbell, W. L. (1996) Calculation of electron paramagnetic resonance spectra from Brownian dynamics trajectories: application to nitroxide side chains in proteins, *Biophys. J. 71*, 2201−2212.
27. Radzwill, N., Gerwert, K., and Steinhoff, H.-J. (2001) Time-resolved detection of transient movement of helices F and G in doubly spin-labeled bacteriorhodopsin, *Biophys. J. 80*, 2856−2866.
28. Perozo, E., Cortes, D. M., and Cuello, L. G. (1998) Three-dimensional architecture and gating mechanism of a K^+ channel studied by EPR spectroscopy, *Nat. Struct. Biol. 5*, 459−469.

29. Perozo, E., Cortes, D. M., Sompornisut, P., Kioda, K., and Martinac, B. (2002) Open channel structure of MscL and the gating mechanism of mechanosensitive channels, *Nature 418*, 942−948.
30. Langen, R., Oh, K. J., Cascio, D., and Hubbell, W. L. (2000) Crystal structures of spin labeled T4 Lysozyme mutants: implications for the interpretation of EPR spectra in terms of structure, *Biochemistry 39*, 8396−8405.
31. Busenlehner, L. S., Salomonsson, L., Brzezinski, P., and Armstrong, R. N. (2006) Mapping protein dynamics in catalytic intermediates of the redox-driven proton pump cytochrome c oxidase, *PNAS 103*, 15398−15403.
32. Yoshikawa, S., Shinazawa-Itoh, K., Nakashima, R., Yaono, R., Yamashita, E., Inoue, N., Yao, M., Fei, M. J., Libeu, C. P., Mizushima, T., Yamaguchi, H., Tomizaki, T., and Tsukihara, T. (1998) Redox-coupled. crystal structural changes in bovine heart cytochrome c oxidase, *Science 280*, 1723−1729.
33. Harrenga, A., and Michel, H. (1999) The cytochrome *c* oxidase from *Paracoccus denitrificans* does not change the metal center ligation upon reduction, *J. Biol. Chem. 274*, 33296−33299.

BI062265H